Supporting Information

Image-Guided Radiotherapy Targets Macromolecules through Altering the Tumor Microenvironment

Authors:

Oliver K. Appelbe,[†,‡] Qingbei Zhang,[†,‡] Charles A. Pelizzari,[§] Ralph R. Weichselbaum,[†,§] and Stephen J. Kron*[,†,‡]

Affiliations:

[†] Ludwig Center for Metastasis Research, The University of Chicago, 5758 South Maryland Avenue, MC 9006, Chicago, IL 60637, United States

[‡] Department of Molecular Genetics and Cellular Biology, The University of Chicago, 929 East 57th Street, GCIS W519, Chicago, IL 60637, United States

[§] Department of Radiation and Cellular Oncology, The University of Chicago, 5758 South Maryland Avenue, MC 9006, Chicago, IL 60637, United States

* Stephen J. Kron, The University of Chicago, GCIS W522A, 929 East 57th Street, Chicago, IL 60637, phone - (773) 834-0250, fax - (773) 702-3611, skron@uchicago.edu

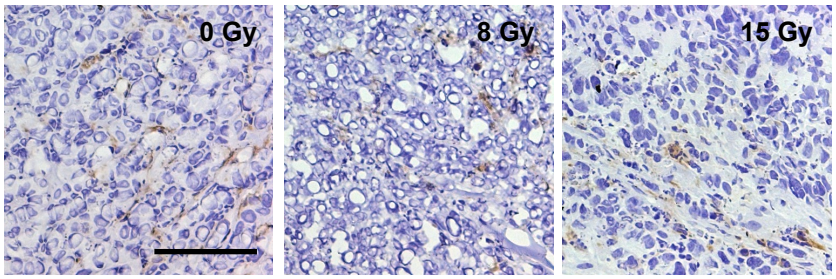

Supplementary Figure 1. Radiation and perivascular apoptosis. Immunohistochemistry of tissue sections of MCF7$^{GFP\text{-}IBD}$ xenograft tumors excised 3 days after irradiation to detect cleaved caspase 3 (brown) displays no marked increase in apoptosis. Scale bar = 200 μm.

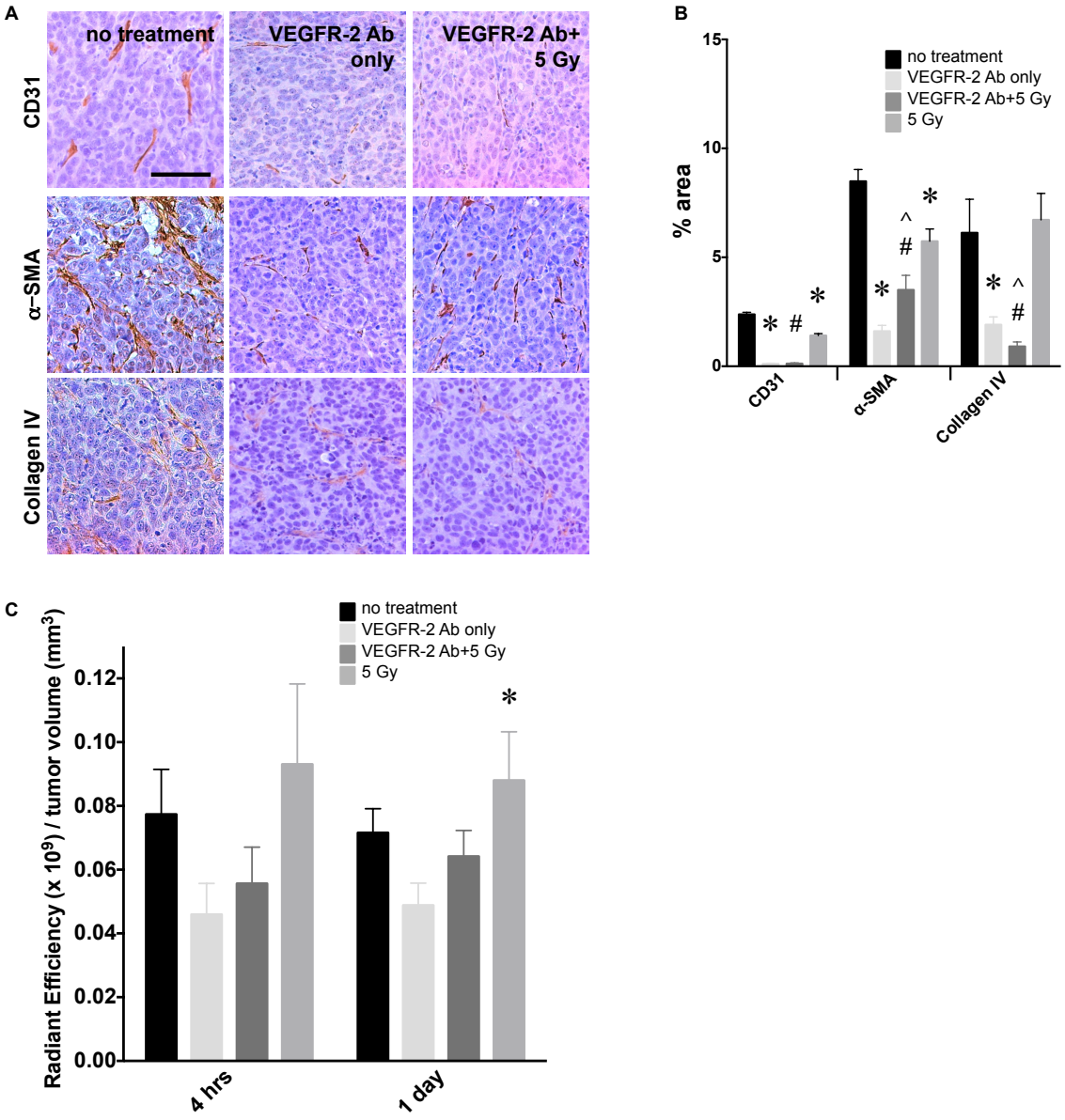

Supplementary Figure 2. VEGFR-2 antibody depletes the tumor endothelium to the detriment of the radiation-enhanced delivery effect. (**A**) Immunohistochemistry of MCF7$^{GFP\text{-}IBD}$ xenograft tumors depicting the decrease in endothelium (CD31, brown), pericytes (α-SMA, brown), and basal lamina (Collagen IV, brown) following treatment with VEGFR-2 antibody. Purple = hematoxylin, nuclei. Scale bar = 200 μm. (**B**)

Relative quantification of IHC staining in $MCF7^{GFP\text{-}IBD}$ tumor sections. % area denotes the area of an image stained calculated using an ImageJ macro (details in methods). * $p \leq 0.05$ relative to no treatment control, # $p \leq 0.05$ relative to 5 Gy only, ^ $p \leq 0.05$ relative to VEGFR-2 antibody only, n = 3. (**C**) $MCF7^{GFP\text{-}IBD}$ tumor retention of AngioSense, measured using IVIS fluorescence quantification, appears limited by the stromal changes apparent following VEGFR-2 treatment. AngioSense was administered 3 days after IR. * $p \leq 0.05$ relative to no treatment control at the same time point, n = 3.

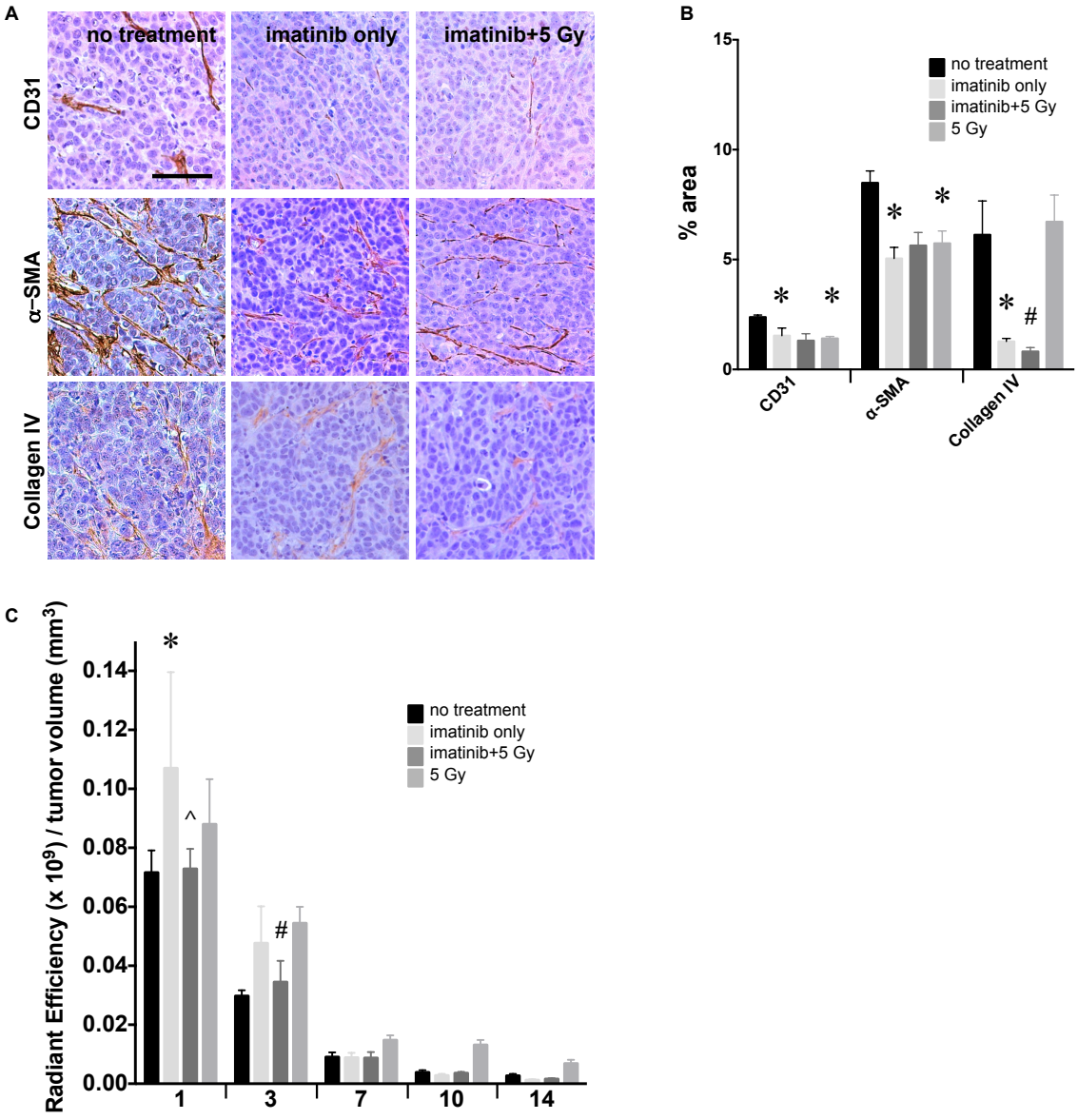

Supplementary Figure 3. Imatinib mesylate treatment leads to depletion of pericytes but does not act synergistically with IR to improve radiation-enhanced accumulation. (**A**) Immunohistochemistry of MCF7$^{GFP\text{-}IBD}$ xenograft tumors depicting the decrease in endothelium (CD31, brown), pericytes (α-SMA, brown), and basal lamina (Collagen IV, brown) following imatinib mesylate treatment. Purple = hematoxylin, nuclei. Scale bar

= 200 μm. (**B**) Relative quantification of IHC staining in $MCF7^{GFP\text{-}IBD}$ tumor sections. % area denotes the area of an image stained calculated using an ImageJ macro (details in methods). * $p \leq 0.05$ relative to no treatment control, # $p \leq 0.05$ relative to 5 Gy only, n = 3. (**C**) $MCF7^{GFP\text{-}IBD}$ tumor retention of AngioSense, measured using IVIS fluorescence quantification, is increased following treatment with imatinib mesylate alone, but not in conjunction with 5 Gy IR. AngioSense was administered 3 days after IR. * $p \leq 0.05$ relative to no treatment control, # $p \leq 0.05$ relative to 5 Gy only, ^ $p \leq 0.05$ relative to imatinib mesylate only, at the same time point, n = 5.

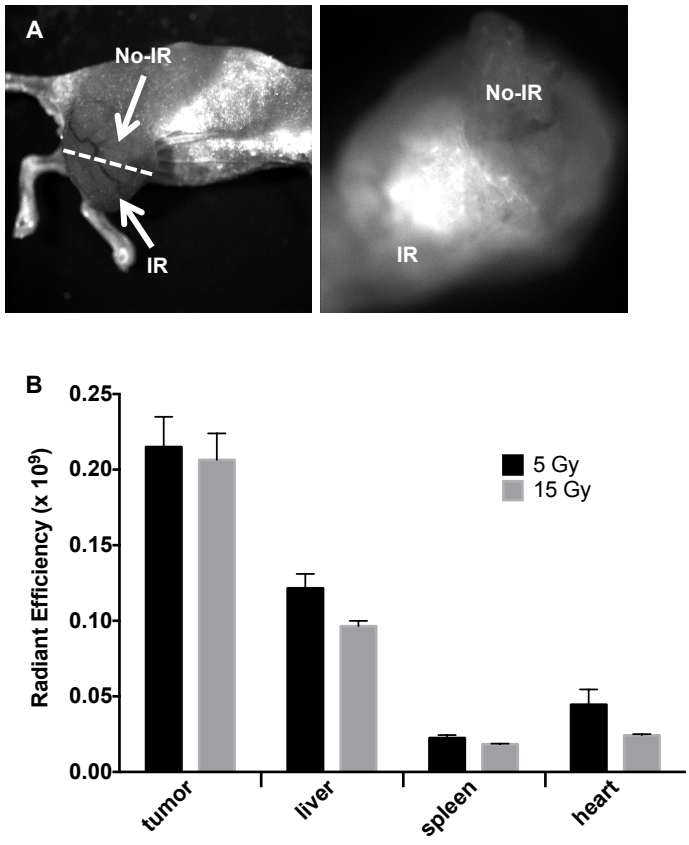

Supplementary Figure 4. Preferential retention of Doxil in irradiated areas of tumors compared to other tissues. (**A**) MCF7$^{GFP\text{-}IBD}$ tumors (prior to Doxil injection, left panel), half irradiated in order to use the unirradiated half as a control, were administered Doxil (10mg/kg) with radiation-enhanced delivery leading to greater drug distribution in the 15 Gy-treated half (right panel). (**B**) Tissue retention of Doxil 26 days after i.v. administration in BALB/c female mice with TUBO hindlimb tumors. Doxil (10 mg/kg) was administered three days following tumor irradiation. n = 2 for each data set.